Fabrication of high aspect ratio TiO_2 and Al_2O_3 nanogratings by atomic layer deposition

Shkondin, Evgeniy; Takayama, Osamu; Michael-Lindhard, Jonas; Larsen, Pernille Voss; Mar, Mikkel Dysseholm; Jensen, Flemming; Lavrinenko, Andrei

Published in:
Journal of Vacuum Science & Technology. A. Vacuum, Surfaces, and Films

Link to article, DOI:
10.1116/1.4947586

Publication date:
2016

Document Version
Publisher's PDF, also known as Version of record

JVSTA Journal of Vacuum Science & Technology A

Fabrication of high aspect ratio TiO2 and Al2O3 nanogratings by atomic layer deposition

Evgeniy Shkondin, Osamu Takayama, Jonas Michael Lindhard, Pernille Voss Larsen, Mikkel Dysseholm Mar, Flemming Jensen, and Andrei V. Lavrinenko

Citation: Journal of Vacuum Science & Technology A **34**, 031605 (2016); doi: 10.1116/1.4947586
View online: http://dx.doi.org/10.1116/1.4947586
View Table of Contents: http://scitation.aip.org/content/avs/journal/jvsta/34/3?ver=pdfcov
Published by the AVS: Science & Technology of Materials, Interfaces, and Processing

Fabrication of high aspect ratio TiO_2 and Al_2O_3 nanogratings by atomic layer deposition

Evgeniy Shkondin[a)]
Department of Photonics Engineering, Technical University of Denmark, DK-2800 Kongens Lyngby, Denmark and Danish National Center for Micro- and Nanofabrication (DANCHIP), DK-2800 Kongens Lyngby, Denmark

Osamu Takayama
Department of Photonics Engineering, Technical University of Denmark, DK-2800 Kongens Lyngby, Denmark

Jonas Michael Lindhard, Pernille Voss Larsen, Mikkel Dysseholm Mar, and Flemming Jensen
Danish National Center for Micro- and Nanofabrication (DANCHIP), DK-2800 Kongens Lyngby, Denmark

Andrei V. Lavrinenko
Department of Photonics Engineering, Technical University of Denmark, DK-2800 Kongens Lyngby, Denmark

(Received 21 February 2016; accepted 14 April 2016; published 28 April 2016)

The authors report on the fabrication of TiO_2 and Al_2O_3 nanostructured gratings with an aspect ratio of up to 50. The gratings were made by a combination of atomic layer deposition (ALD) and dry etch techniques. The workflow included fabrication of a Si template using deep reactive ion etching followed by ALD of TiO_2 or Al_2O_3. Then, the template was etched away using SF_6 in an inductively coupled plasma tool, which resulted in the formation of isolated ALD coatings, thereby achieving high aspect ratio grating structures. SF_6 plasma removes silicon selectively without any observable influence on TiO_2 or Al_2O_3, thus revealing high selectivity throughout the fabrication. Scanning electron microscopy was used to analyze every fabrication step. Due to nonreleased stress in the ALD coatings, the top parts of the gratings were observed to bend inward as the Si template was removed, thus resulting in a gradual change in the pitch value of the structures. The pitch on top of the gratings is 400 nm, and it gradually reduces to 200 nm at the bottom. The form of the bending can be reshaped by Ar^+ ion beam etching. The chemical purity of the ALD grown materials was analyzed by x-ray photoelectron spectroscopy. The approach presented opens the possibility to fabricate high quality optical metamaterials and functional nanostructures. © *2016 American Vacuum Society*. [http://dx.doi.org/10.1116/1.4947586]

I. INTRODUCTION

This work presents the fabrication of periodic nanostructured gratings of TiO_2 and Al_2O_3 with an aspect ratio up to 50 and demonstrates controllable highly selective etching of Si during the TiO_2 and Al_2O_3 grating formation. The procedure combines dry etch and atomic layer deposition (ALD) techniques. ALD is a self-limiting surface reaction method based on sequential and separate introduction of two precursors.[1] Through a repeated cyclic exposure, a thin film is slowly deposited. This is the only technique that allows the deposition of extremely conformal coatings on complex three-dimensional nanostructures.[1] ALD of TiO_2 and Al_2O_3 has been intensively studied and heavily implemented in a variety of applications in physics.[2–10]

In recent years, the theoretical advances in nanophotonics impose a great demand on developing fabrication techniques that allow patterning of high quality optical materials on nanoscale.[11] High aspect ratio trench structures can serve as one-dimensional photonic crystals (1D PhCs) as an alternative to conventional thin-film multilayers in a vertical strata arrangement. A photonic crystal consisting of a periodic arrangement of high and low refractive index media possesses a photonic bandgap, where light within a certain wavelength range is prohibited to propagate.[12] 1D PhCs by definition have no complete bandgaps opened in all directions inside the structure. Nevertheless, in the reduced space of the wavevectors inside the structure, a PhC may exhibit a unique property of the omnidirectional reflection of external radiation.[12,13] Such a structure serves, for example, as a bandpass filter.[14] Previously, high aspect ratio vertical 1D PhCs have been realized as Si trench structures and studied for telecommunication wavelengths of around 1.5 μm where Si is transparent.[15,16] However, Si is not transparent in the visible wavelength region. Therefore, 1D PhCs made of TiO_2 and Al_2O_3 are desirable candidates for applications in the visible and near-infrared regimes. Moreover, the capability to deposit thin films in a conformal way on trench structures can effectively tune a stopband. Such tuning of a photonic bandgap by a third layer (SiO_2) has been performed by oxidizing the surface of Si.[17] Fabrication of photonic crystals by ALD can also be applied toward realization of two dimensional PhCs (Ref. 18) as well as other kinds of structured functional materials such as epsilon-near-zero metamaterials.[19] In addition to the advanced deposition of dielectric layers, the deposition capability of metals [e.g., Cu (Ref. 20)] and conductive oxides, [e.g., aluminum-doped

[a)]Electronic mail: eves@fotonik.dtu.dk

ZnO (Ref. 21)] also provides fabrication flexibility for demands of metamaterials with metal or metallic-like components. Apart from the telecommunication applications, high aspect-ratio vertical 1D PhCs can find various applications ranging from color filters[22] to optofluidic sensors for biosensing. In the latter case, liquid flows through trenches, and the refractive index of the liquid is analyzed by a shift of a photonic bandgap.[23]

In contrast to vertical silicon trenches, the high aspect ratio structures in oxides such as TiO_2 and Al_2O_3 cannot be patterned in the same way by conventional methods such as reactive ion etching (RIE). A recent paper by Huang *et al.*[18] proposed a new method to pattern TiO_2. In this approach, ALD has a key role, since patterning formation is based on deposition rather than etching the desired material. The main idea in this method is based on three steps: (1) fabrication of a Si template which is coated by an ALD-deposited film, (2) the ALD film is partially removed by plasma etching techniques, which provides an open access to the original Si template core, and (3) the template is etched away leaving the ALD coated structure with an advance topology. Such a procedure requires high selectivity during the back etching of the template.

II. EXPERIMENT

All the samples were prepared and characterized in a class 100 cleanroom. Si (100) wafers of 150 mm were used as a substrate. The main steps in the gratings manufacturing are shown in Fig. 1. First, the silicon trenches were realized by deep reactive ion etching (DRIE) [Fig. 1(a)]. Then, the trenches were ALD coated [Fig. 1(b)]. After the selective removal of the top parts [Fig. 1(c)], the silicon core between ALD coatings was etched away during the last step. Figure 1(d) represents the final structure, which is the highly anisotropic vertical grating. Each fabrication step was carefully evaluated using cross-sectional scanning electron microscopy (SEM) imaging.

A. Template fabrication

Conventional deep-UV lithography was implemented for defining the grating pattern. The normal procedure includes bottom antireflective coating (BARC) and photoresist coating followed by spray development. To promote adhesion and minimize interference effects, the substrate surface was coated with a 65 nm thick BARC coating (DUV42S-6, Brewer Science, USA) followed by a bake-out at 175 °C for 60 s. The positive photoresist (KRF M230Y, JSR Micro, NV) was spin-coated to a thickness of 360 nm and baked at 130 °C for 90 s. A pitch of 400 nm was chosen for the gratings. The resist was exposed in a Canon FPA-3000 EX4 DUV stepper on field sizes of $2 \times 2\,cm^2$. In the next step, the silicon trenches were prepared using an advanced DRIE technique.[23] Three main steps were used in the Si trench fabrication: etching of the BARC layer, selective silicon etching, and resist removal. The BARC etching step proceeded for 1 min using 40 sccm of oxygen plasma with coil and platen powers of 400 and 20 W, respectively. In the DRIE silicon etch, a Bosch process[24] was implemented, where the etching was done by repetitive steps of surface passivation and etching for 2.5 and 5 s, respectively, with a process

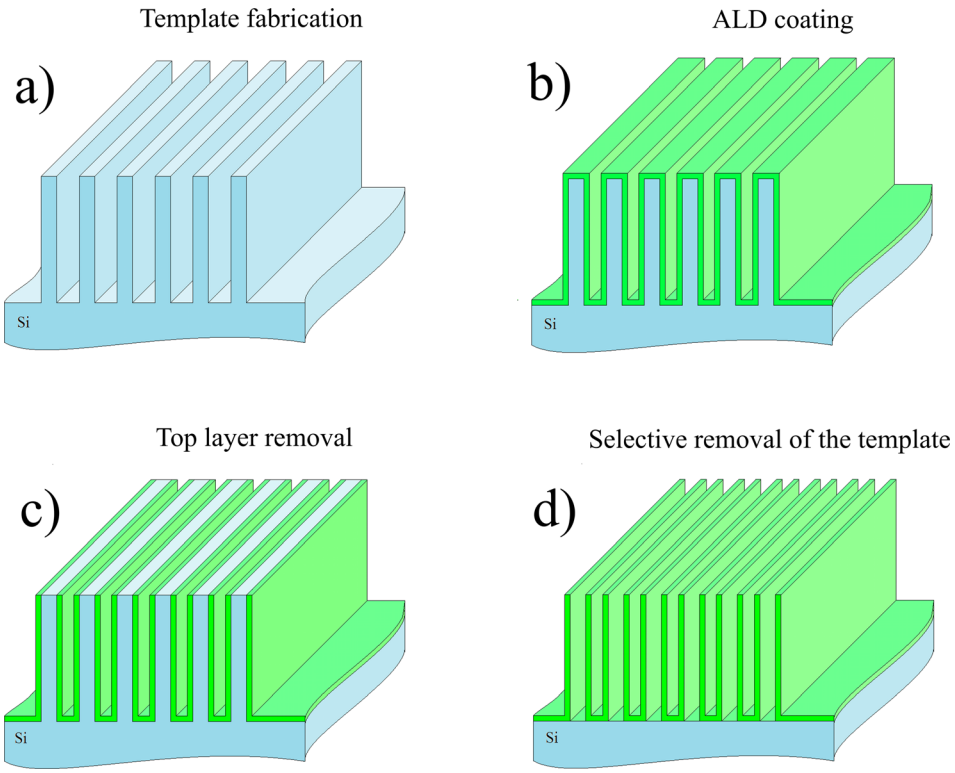

FIG. 1. (Color online) Scheme of fabrication flow. (a) Fabrication of trenches in silicon using DRIE. (b) Atomic layer deposited TiO_2 or Al_2O_3 coatings. (c) Selective removal of the top part. (d) Isolation of the coatings by silicon etching.

TABLE I. DRIE parameters for Si trench fabrication.

		Passivation (5 s)	Etching (2.5 s)
Process gas flow (sccm)	C_4F_8	50	20
	SF_6	—	60
	O_2	—	5
Powers (W)	Coil	600	400
	Platen	—	40

pressure of 10 mTorr. The processing substrate temperature was kept at 20 °C. Table I summarizes the process parameters.

The depth of the trenches was controlled by adjusting the number of cycles. In this work, this depth was kept at 4.5 μm, which with the present etching conditions corresponded to 70 cycles.

The last step in the Si trench fabrication was the removal of the mask photoresist using oxygen plasma for 2 min with a flow of 100 sccm and coil and platen powers of 800 and 20 W, respectively. The depth, pitch, and general shape of the silicon trenches were confirmed by cross-section SEM investigation [Fig. 2(a)].

B. Atomic layer deposition

The TiO_2 and Al_2O_3 coatings were made in a hot-wall ALD system (Picosun R200). The precursors used for TiO_2 and Al_2O_3 deposition were titanium tetrachloride ($TiCl_4$) and trimethylaluminum $Al(CH_3)_3$, respectively (supplied by Sigma Aldrich). Deionized water was used as oxidant source in both processes. In the case of TiO_2 deposition, the temperature of 150 °C was chosen in order to minimize the TiO_2 surface roughness caused by crystalline anatase transition known to occur at high temperatures.[25] The growth rates of TiO_2 and Al_2O_3 coatings were found to be 0.045 and 0.089 nm/cycle, respectively, (in agreement with the previously reported data[26]) using varying-cycles deposition with ellipsometric characterization of the film thicknesses and refractive indices (VASE, J.A. Woollam Co.). No significant variations of deposition rates were observed. ALD recipes for TiO_2 and Al_2O_3 are represented in Tables II and III. The same precursor was introduced twice into the chamber in order to ensure successful diffusion to the bottom of the trenches. In order to grow 90 nm coatings, 2000 and 1000 cycles were used for TiO_2 and Al_2O_3, respectively. Figure 2(b) shows a cross-section SEM micrograph, which reveals the high quality conformal coatings.

C. Removal of the top part and template back etching

The top TiO_2 and Al_2O_3 layers were removed by inductive coupled plasma (ICP). Etching of TiO_2 and Al_2O_3 in ICP systems were previously reported,[27,28] especially etch of Al_2O_3 received attention due to its beneficial use as a hard mask and a gate dielectric.[28] In the case of TiO_2, a Cl_2 flow was used. The removal of Al_2O_3 involved BCl_3 and Cl_2. First, the removal of TiO_2 and Al_2O_3 was investigated on planar Si substrates. Al_2O_3 of 145 nm and 90 nm of TiO_2 were deposited on silicon and etched using recipes described in Table IV. The remaining thickness of deposited layers was measured using spectroscopic ellipsometry versus process time. The results are summarized in Figs. 3(a) and 3(b). The etch rates of TiO_2 and Al_2O_3 following these recipes are

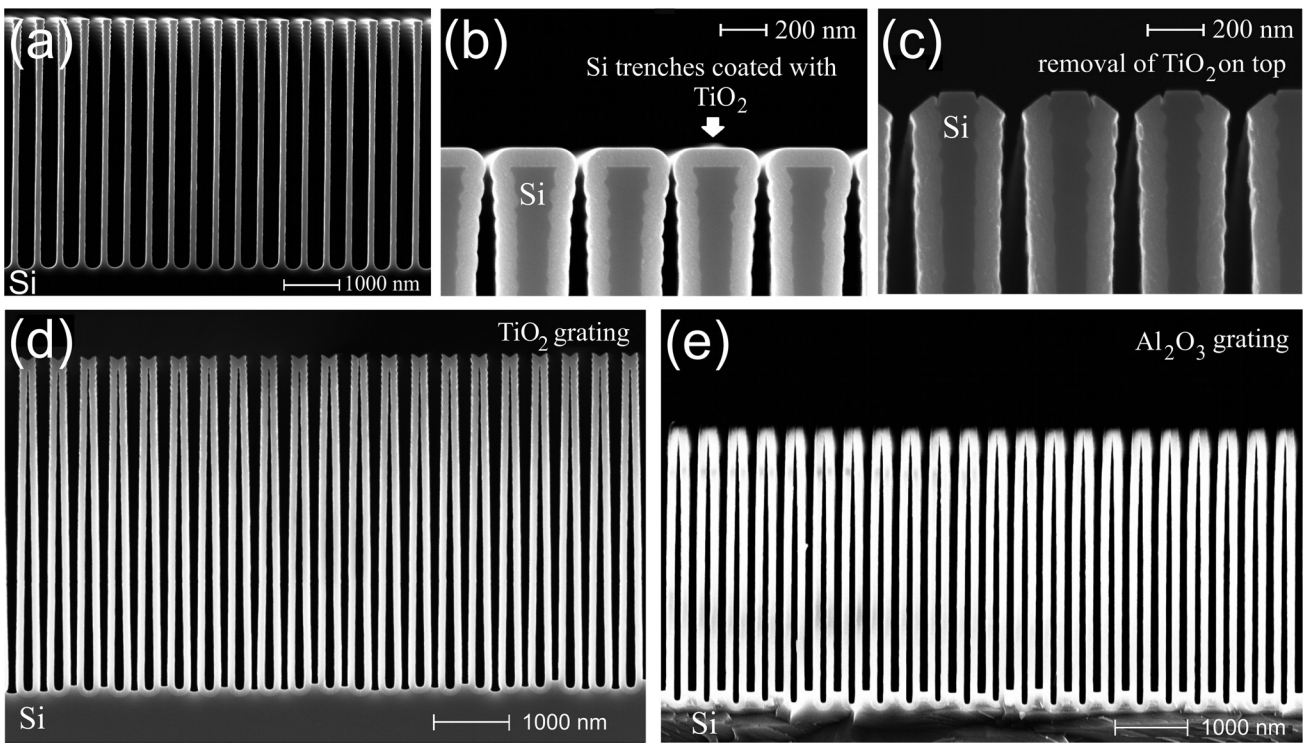

FIG. 2. (a) Fabricated silicon trenches. (b) ALD coating of TiO_2. (c) Selective opening of the top parts of the gratings. (d) Fabricated TiO_2 and (e) Al_2O_3 gratings.

TABLE II. Recipe for one cycle of TiO_2.

Precursor	Carrier gas flow (sccm)	Pulse (s)	Purge (s)
$TiCl_4$	150	0.1	0.5
$TiCl_4$	150	0.1	20
H_2O	200	0.1	0.5
H_2O	200	0.1	20

0.11 and 0.89 nm/s, respectively. It is important to strictly control the etching of the top part of TiO_2 and Al_2O_3 since an overetch can damage the silicon core beneath the ALD coatings and the control of the grating fabrication can be lost, due to the fact that the depth of the Si core will become unknown. The TiO_2 grating after removal of the top part but still with the Si template can be seen in Fig. 2(c).

The subsequent selective silicon etching (template removal) proceeded using a continuous isotropic silicon etch in the ICP etch system based on SF_6 at a substrate temperature of 20 °C. This process exhibit an extreme selectivity with respect to oxides and selectivity of Si to Al_2O_3 was previously reported to be 66 000:1 in SF_6 ICP plasma.[29] Table IV summarizes the process. Figure 3(c) shows the etch depth as a function of time. Controlling the time is essential, since overetching will lead to collapse of the gratings. The coil power can be reduced in order to slow down silicon etching. However, reducing it below 300 W results in nonuniform etching across the sample. Figures 2(d) and 2(e) show SEM cross-sections of the fabricated nanostructured TiO_2 and Al_2O_3 gratings.

III. RESULTS AND DISCUSSION

The TiO_2 and Al_2O_3 nanostructured gratings were successfully grown and isolated on the Si substrates. The SEM cross-section investigation [Figs. 2(a)–2(e)] reveals high selectivity and precise control in all steps throughout the fabrication. With the thickness of Al_2O_3/TiO_2 coatings of 90 nm and gratings height of 4500 nm, the aspect ratio of the fabricated nanostructures is 1:50.

During DRIE, the substrate suffers from the scallops formed during the first 5–10 etching cycles. These scallops are typical for the Bosh etch process,[24] and cause the undesired roughness of the subsequent ALD coatings. After these first DRIE cycles, the etching proceeds smoothly with only a very small variation of the Si trench width. The thickness of the fabricated Si walls at the bottom is 100 nm, while at the very top 150 nm. The variation of the wall thickness mainly occurs during DRIE of the first micrometer depth.

TABLE III. Recipe for one cycle of Al_2O_3.

Precursor	Carrier gas flow (sccm)	Pulse (s)	Purge (s)
TMA[a]	150	0.1	0.5
TMA	150	0.1	20
H_2O	200	0.1	0.5
H_2O	200	0.1	20

[a]Trimethylaluminum, $Al(CH_3)_3$

TABLE IV. Recipes for Al_2O_3, TiO_2, and Si in ICP etch system.

Process parameters[a]	TiO_2 etch	Al_2O_3 etch	Si etch
Cl_2 (sccm)	30	1.2	—
BCl_3 (sccm)	—	6.8	—
SF_6 (sccm)	—	—	90
Pressure (mTorr)	3	4	10
Coil power (W)	900	1200	400
Platen power (W)	50	200	3

[a]Process temperature is 20 °C for all processes.

ALD of 90 nm Al_2O_3 and TiO_2 revealed very high quality layers with no noticeable variation in thickness, despite the very high aspect ratio of DRIE etched Si trenches.

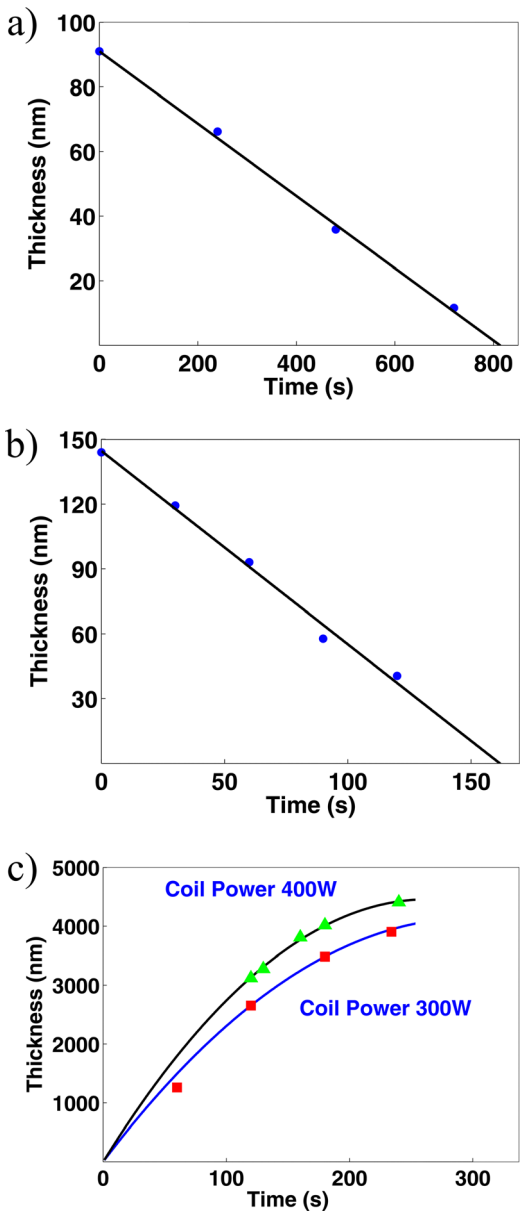

FIG. 3. (Color online) Etch rate measurements of ALD layers on planar Si substrates for (a) TiO_2 using Cl_2 based etching and (b) Al_2O_3 using Cl_2/BCl_3 based etching, respectively. (c) Depth of silicon vs time during Si template removal in ICP using SF_6.

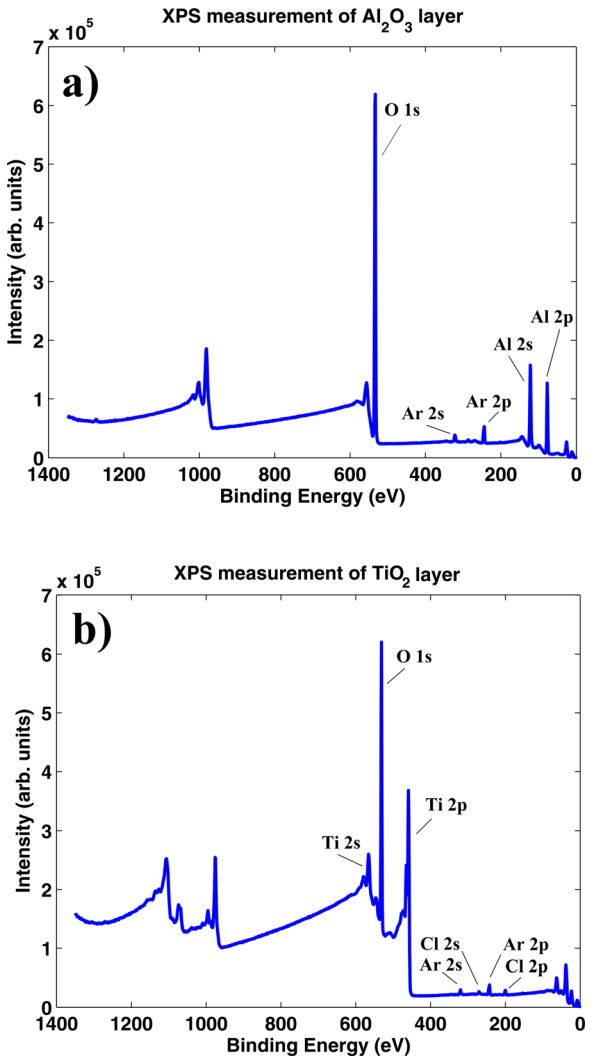

FIG. 4. (Color online) XPS measurements of ALD of (a) TiO_2 and (b) Al_2O_3 on planar Si substrates. The surfaces of the samples were cleaned with Ar^+ ions for 10 s prior the measurements. Case (b) reveals a small (1–3 at. %) amount of Cl_2 incorporated into TiO_2 sample.

For evaluating the chemical composition, ALD of TiO_2 and Al_2O_3 was made on planar Si substrates. The planar structures were analyzed by x-ray photoelectron spectroscopy (XPS) in order to detect possible impurities in the chemical composition (Fig. 4). Al_2O_3 samples revealed chemically high quality films with no observable contaminations [Fig. 4(a)], whereas the TiO_2 film contained around 2–3 at. % of chlorine residuals, which originate from the unreacted $TiCl_4$ precursor [Fig. 4(b)]. The presence of chlorine can be reduced to below the detection level of the XPS measurement at ALD growth temperatures around 300 °C. However, such high growth temperatures lead to the crystalline anatase phase transition, which will heavily increase coating roughness.[30] Chlorine free precursors such as Titaniumtetraisopropoxide (TTIP)[31] must be considered as an alternative for ALD of TiO_2 at 150 °C and below.

The removal of the top part has to be done with care since the silicon beneath the TiO_2 and Al_2O_3 coatings immediately will start to be etched by the Cl_2 or Cl_2/BCl_3 based plasma. The back etch of the original silicon template using the isotropic dry etching recipe based on continuous SF_6 process shows no significant height differences of the fabricated gratings across the sample. This process, however, is nonlinear and very sensitive to the coil power of the ICP tool [Fig. 3(c)]. A coil power of 400 W was the most optimum, since decreasing below 300 W leads to larger deviations of the height of the remaining Si core and increasing above 400 W results in a higher etching speed and less control of the etching conditions. The nonlinearity during Si core removal represented in Fig. 3(c) puts a demand on controlling the condition during the previous TiO_2/Al_2O_3 top opening step. During silicon etching between the ALD coating steps, no influence on the TiO_2/Al_2O_3 thin film morphology has been observed as a result of the very selective Si etch. This is a rather significant result since it opens the opportunity to fabricate similar structures using other materials by using the right chemical selectivity and the possibility of ALD growth. The fabricated Al_2O_3 and TiO_2 gratings have a shape similar to the surface of the original Si template. Due to the highly conformal nature of the ALD growth, the shape of the scallops from the silicon template is transferred to the ALD grown gratings.

This initial roughness together with the fact that the ALD films are grown at elevated temperature, while the silicon template removal between ALD coatings occurs at room temperature, leads to an outward bending of the top grating parts. This bending is caused by the built-in stress and was observed on both TiO_2 and Al_2O_3 gratings. This is the main drawback of the above described experimental approach. The reason for the bending is that ALD is a thermally activated process, and in this case, the deposition was carried out at 150 °C, while the Si back etching in the ICP etcher proceeded at 20 °C. The accumulated stress is released during the silicon removal. Indeed, Al_2O_3 and TiO_2 have thermal expansion coefficients 8.2×10^{-6} °C^{-1} and 9×10^{-6} °C^{-1}, respectively, while for Si this parameter is much less (2.6×10^{-6} °C^{-1}). The difference in thermal expansion between oxides and silicon is the reason why the oxide coatings tend to bend outward and get attached to their neighbors during Si template removal. Nevertheless, the bending features are perfectly periodic, which allow for improvements of the top part. One way of improvement is ion beam etching using Ar^+ ions. This will allow to shape the fabricated gratings with the "fence" profile as shown in Figs. 5(a) and 5(b), for a grating that has now a pitch of the original one 400 nm with small gap between coatings.

IV. SUMMARY AND CONCLUSIONS

To summarize, vertically nanostructured TiO_2 and Al_2O_3 gratings were fabricated. The present work demonstrates the powerful combination of conformal ALD growth of dielectric layers on a high aspect ratio Si template and subsequent highly selective etching of the Si template. Silicon etching is an isotropic process which makes it extremely flexible to the realization of different types of 3D ALD structures such as trenches, pillars, pores, etc. Combining DRIE and ALD, it is possible to create vertical oxides nanogratings with such a high aspect ratio, which is not possible to obtain by any other

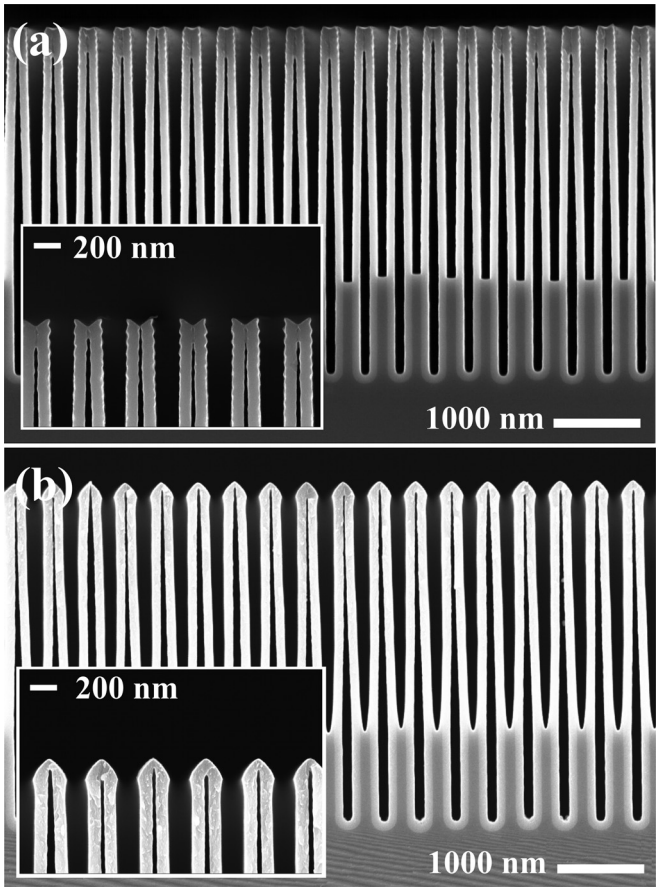

FIG. 5. Shaping the top part of fabricated gratings by the "fence" profile. (a) Fabricated TiO_2 grating. (b) Shaping the top part of TiO_2 grating profile using Ar^+ IBE. The insets show magnified pictures.

technique. Additionally, it is also possible to create high ratio ternary compounds such as $Al_xTi_yO_z$, with different constituent concentrations by varying TMA and $TiCl_4$ cycles in the ALD recipes.[32] It will allow the tailoring of the effective refractive index of gratings. Periodic structures of other materials, which are known for their difficulties in patterning such as ZnO, can also be tested for realization. Realized structures can be further improved by Ar^+ ion beam etching which allows tuning the top part of the gratings, minimizing their roughness and changing the top shape. The well-defined high aspect ratio trench structure made of Al_2O_3 and TiO_2 are good candidates for 1D PhCs in the visible and near infrared regions. Furthermore, combined with other materials that can be deposited by ALD such as ZnO and Cu, the trench structures can serve as a generic platform for different types of metamaterials possessing extravagant optical properties.

As for the outlook, further work is needed on the top separation of the gratings lamina. This should be handled in combination with development of new DRIE recipes with more direct wall profiles, without pronounced roughness and scallops and improved ALD conditions.

ACKNOWLEDGMENTS

The authors would like to thank process specialists from Danish National Center for Micro- and Nanofabrication (DANCHIP) E. Khomtchenko and M. Keil for all work related to deep UV lithography. The authors acknowledge P. Shi for fruitful discussions and practical recommendations and R. Malureanu, A. Andryieuski, and S. Zhukovsky for the ideas related to possible output of grating structures.

[1]S. M. George, Chem. Rev. **110**, 111 (2010).
[2]G. Dingemans and W. M. M. Kessels, J. Vac. Sci. Technol., A **30**, 040802 (2012).
[3]K. Henkel, B. Seime, I. Paloumpa, K. Müller, and D. Schmeißer, IOP Conf. Ser. Mater. Sci. Eng. **8**, 012036 (2010).
[4]S. E. Potts *et al.*, J. Electrochem. Soc. **158**, C132 (2011).
[5]M. Tallarida, M. Weisheit, K. Kolanek, M. Michling, H. J. Engelmann, and D. Schmeisser, J. Nanoparticle Res. **13**, 5975 (2011).
[6]C. Marichy, N. Donato, M. Latino, M. Georg Willinger, J.-P. Tessonnier, G. Neri, and N. Pinna, Nanotechnology **26**, 024004 (2015).
[7]I.-S. Yu, Y.-W. Wang, H.-E. Cheng, Z.-P. Yang, and C.-T. Lin, Int. J. Photoenergy **2013**, 431614 (2013).
[8]E. Jardinier, G. Pandraud, M. H. Pham, P. J. French, and P. M. Sarro, J. Phys. Conf. Ser. **187**, 012043 (2009).
[9]A. L. Linsebigler, J. T. Yates, Jr., G. Lu, G. Lu, and J. T. Yates, Chem. Rev. **95**, 735 (1995).
[10]A. Rissanen and R. L. Puurunen, Proc. SPIE **8249**, 82491A (2012).
[11]W. Cai and V. Shalaev, *Optical Metamaterials: Fundamentals and Applications* (Springer-Verlag, New York, 2010).
[12]J. J. D. Joannopoulos, S. Johnson, J. N. J. Winn, and R. R. D. Meade, *Photonic Crystals: Molding the Flow of Light* (Princeton University, NJ, 2008).
[13]D. N. Chigrin, A. V. Lavrinenko, D. A. Yarotsky, and S. V. Gaponenko, Appl. Phys. A **68**, 25 (1999).
[14]V. A. Tolmachev, A. V. Baldycheva, S. A. Dyakov, K. Berwick, and T. S. Perova, J. Lightwave Technol. **28**, 1521 (2010).
[15]V. A. Tolmachev, E. V. Astrova, J. A. Pilyugina, T. S. Perova, R. A. Moore, and J. K. Vij, Opt. Mater. **27**, 831 (2005).
[16]G. Barillaro, L. Marsilio Strambini, V. Annovazzi-Lodi, and S. Merlo, IEEE J. Sel. Top. Quantum Electron. **15**, 1359 (2009).
[17]A. Baldycheva, V. A. Tolmachev, T. S. Perova, Y. A. Zharova, E. V. Astrova, and K. Berwick, Opt. Lett. **36**, 1854 (2011).
[18]Y. Huang, G. Pandraud, and P. M. Sarro, Nanotechnology **23**, 485306 (2012).
[19]P. Moitra, Y. Yang, Z. Anderson, I. I. Kravchenko, D. P. Briggs, and J. Valentine, Nat. Photonics **7**, 791 (2013).
[20]B. H. Lee *et al.*, Angew. Chem. Int. Ed. **48**, 4536 (2009).
[21]T. Dhakal, D. Vanhart, R. Christian, A. Nandur, A. Sharma, and C. R. Westgate, J. Vac. Sci. Technol. **30**, 021202 (2012).
[22]E.-H. Cho *et al.*, Opt. Express **17**, 8621 (2009).
[23]S. Surdo, S. Merlo, F. Carpignano, L. M. Strambini, C. Trono, A. Giannetti, F. Baldini, and G. Barillaro, Lab Chip **12**, 4403 (2012).
[24]V. Lindroos, M. Tilli, A. Lehto, T. Motooka, and T. Veijola, *Handbook of Silicon Based MEMS Materials and Technologies* (William Andrew Publishing, Norwich, NY, 2010).
[25]W. J. Lee and M.-H. Hon, J. Phys. Chem. C **114**, 6917 (2010).
[26]D. R. G. Mitchell, D. J. Attard, K. S. Finnie, G. Triani, C. J. Barbé, C. Depagne, and J. R. Bartlett, Appl. Surf. Sci. **243**, 265 (2005).
[27]J. Woo, Y. Chun, Y. Joo, and C. Kim, Vaccum **86**, 2152 (2012).
[28]S. Tegen and P. Moll, J. Electrochem. Soc. **152**, G271 (2005).
[29]L. Sainiemi and S. Franssila, J. Vac. Sci. Technol., B **25**, 801 (2007).
[30]Y. Huang, G. Pandraud, and P. M. Sarro, J. Vac. Sci. Technol. A **31**, 01A148 (2013).
[31]B. Hudec *et al.*, Microelectron. Eng. **88**, 1514 (2011).
[32]A. P. Alekhin, A. A. Chouprik, S. A. Gudkova, A. M. Markeev, Y. Y. Lebedinskii, Y. A. Matveyev, and A. V. Zenkevich, J. Vac. Sci. Technol., B **29**, 01A302 (2011).